Numerical Methods in Civil Engineering

Prediction of Groundwater Fluctuations Using Meshless Local Petrov-Galerkin Numerical Method in a Field Aquifer (Birjand Aquifer)

Ali Mohtashami[*], Seyed Arman Hashemi Monfared[**], Gholamreza Azizyan[***], Abolfazl Akbarpour[****]

ARTICLE INFO

Article history:
Received:
January 2019.
Revised:
March 2019.
Accepted:
April 2019.

Keywords:
Groundwater
Water level estimation
Modeling
Meshless local Petrov-Galerkin method
Birjand
Iran.

Abstract:

The prediction of groundwater level fluctuations is one of the most remarkable issues in water resources management, especially in arid and semiarid regions. The present study uses a numerical meshless method, named meshless local Petrov-Galerkin, to predict the groundwater level over a ten-year period. This method makes up for the shortcomings of mesh-dependent methods and increases modeling accuracy significantly. The study site is the unconfined aquifer of the Birjand plain with 190 groundwater discharge wells. The groundwater head is predicted based on two scenarios. The first scenario is defined as the discharge rate increased by 10% compared to the year before. Due to this scenario, the groundwater level in the aquifer is significantly reduced, especially in the central part (in the location of piezometer No. 8) and southwestern part (in the location of piezometer No. 5) of the aquifer, where groundwater table experiences 11.74 m and 35.80 m drawdown, respectively over a 10-year period. In that area, the high density of groundwater wells is the main reason for the depletion of the aquifer. Within the second scenario, the effect of rainfall rate is assessed by decreasing it by 20% and increasing discharge rate of groundwater wells by 5% compared to the year before. The results of this scenario show that the declines of groundwater level in the southwestern and central parts of the aquifer around 14.81 m and 5.05 m, respectively during the considered ten-year period.

1. Introduction

Groundwater is one of the main sources of water supply for industrial, drinking, and agricultural purposes. This resource constitutes the only source of water supply in many arid and semi-arid regions all over the world. Even in countries with high (above-average) precipitation rate, groundwater is still the primary water resource due to its availability [1]. The overuse of this water resource due to the population growth and the development of urbanization and industry has significantly lowered groundwater levels and has caused the rapid depletion of aquifers [2].

** Ph. D. student, , Faculty of Eng., Civil Engineering Dep., University of Sistan and Baluchestan, Zahedan, Iran.*
*** Coresponding Author: Associate Professor, Civil Eng. Dep., University of Sistan and Baluchestan, Zahedan, Iran. Email: hashemi@eng.usb.ac.ir*
**** Associate Professor, Civil Eng. Dep., University of Sistan and Baluchestan, Zahedan, Iran.*
***** Associate Professor, Civil Eng. Dep., University of Birjand, Birjand, Iran.*

Therefore, it is necessary to accurately simulate and predict the behavior of aquifers and the fluctuation of groundwater tables. Prediction is one of the main strategies to reduce the destructive effects of over-extraction of groundwater and can help water resources managers, decision makers, and planners to achieve their goals [3, 4].

Nowadays, researchers use different numerical methods to analyze groundwater flow [5]. Mostly, the finite difference method and the finite element method, which were implemented in GMS and FeFlow software packages, respectively have been used for this purpose. Recently, another numerical method, named meshless method, was used as well [6]. High accuracy and easy access to its open-source code are two advantages of this method that make it more popular than other numerical methods. Among the meshless methods, the meshless local Petrov-Galerkin method has widely been used in the field of fluids, especially groundwater [7]. For example, Mohtashami et al. 2017 [7,

8] estimated groundwater head in a real unconfined aquifer both in the steady state and unsteady state using the meshless local Petrov-Galerkin method and compared the results with the results of finite difference method. The higher accuracy of the results of the meshless method shows its better performance, which can be used to predict groundwater levels more reliably and efficiently. Several studies, which have predicted groundwater level fluctuations, are presented below.

Wen et al. (2007)[9] modeled the Zhangye aquifer in northwestern China by finite element method and analyzed groundwater flow. After calibration and validation of the model using the data for 1994-2000, groundwater level in this aquifer was predicted with two scenarios for the thirty-year period of 2000-2030. With the first scenario, the groundwater abstraction remains steady until 2030. With the second scenario, the groundwater abstraction was reduced over the same period. The results showed that with the first scenario, the predicted maximum drawdown was 30 m in the south of the aquifer in 2030, but with the second scenario, the value and range of the hydraulic head drawdown were less, reaching at a maximum of 24 m in the south of the aquifer in 2030. Shiri et al. (2013)[10] used gene expression programming algorithms, neural fuzzy systems, artificial neural networks, and support vector machines -a relatively novel and promising estimator in data-driven research fields, whose basic concepts and theory were introduced by Cortes and Vapnik (1995) [11]- to predict groundwater level fluctuations. Their model's input data included groundwater level, precipitation and evaporation rates over a 7-year period (2001-2008) for the real Hongcheon aquifer located in South Korea. The groundwater level was predicted for a 7-year period. The results showed that groundwater level went higher slightly during the 7-year period.

Shirmohammadi et al. (2013)[12] predicted groundwater level fluctuations in Mashhad aquifer ,located in Khorasan Razavi province, Iran using the system identification and neural fuzzy system methods. They predicted the groundwater level for two months. Their results showed that the groundwater level increased by around 0.30 m during the investigated period. Emamgholizadeh et al. (2014)[13] predicted groundwater head in Bastam aquifer in Semnan province in Iran using two artificial neural network models and fuzzy neural systems. For this purpose, the nine-year hydrological and geostatistical data including rainfall and pumping rates were introduced as inputs to the model. After modeling, calibrating and validating the model, the groundwater level fluctuations were determined with several scenarios for two years after. The studied scenarios were as follow: (1) The rainfall rate and the recharge rate were assumed constant; (2) the precipitation rate was assumed constant and the pumping rate was decreased by 26%; and (3) the pumping rate remained constant and the precipitation rate increased by 30%.

To predict the groundwater level in Kashmar, Ghaffarian (2013)[14] modeled groundwater flow using GMS software. In his study, groundwater fluctuations were simulated under different conditions. The results showed that under the status quo, the groundwater level would decrease about 1 meter per year. By assuming 10%, 30% and 50% increase in the aquifer discharge rate, the groundwater level would reduce 1.15, 1.50 and 2.20 m, respectively. Nikbakht and Najib (2016)[15] predicted the groundwater level by 1400 for the Ajab Shir aquifer located in East Azarbaijan province, Iran. Firstly, they defined the conceptual model of groundwater using the MODFLOW package, and after calibrating and validating the model, calculated the groundwater balance assuming that the irrigation systems of this plain were changed to the pressurized irrigation system. This change led to saving 3.23 million cubic meter water in the aquifer per year. Furthermore, the groundwater level increased by 4.63 m.

Ghobadian et al. (2016)[16] modeled the groundwater level using GMS (Groundwater Modelling System) software in the Khezel aquifer in Hamadan province, Iran and predicted the groundwater level fluctuations for the 1, 3 and 10 years after, considering two scenarios: (1) the status quo and (2) the scenario of 10% reduction in pumping rate. The results predicted a large drawdown in the northeast part of the aquifer. Yousefi et al. (2016)[17] wrote an open-source code in Matlab software to determine the optimal policies for the extraction of wells in the Karaj aquifer. In this regard, their open-source code was based on the finite difference numerical method. They first modeled the aquifer and after calibrating and validating their model, analyzed groundwater flow and predicted groundwater level over a 10-year period considering three scenarios of the status quo, an optimistic assumption, and a pessimistic assumption. For the status quo, all the input data were constant. With the optimistic assumption, the extraction rate from wells for drinking water was constant, but for the other usages, was reduced by 10 percent. With the pessimistic scenario, the rate of extraction was increased by 1.5 percent per annum. The results showed that in the three studied scenarios, the aquifer experienced drawdowns of 12.83, 4.90 and 17.19m, respectively.

Following the aforementioned studies, the present research investigates the groundwater level in Birjand aquifer considering the following scenarios. One of the most important factors in planning an optimal management scheme for groundwater resources is to have enough knowledge and information about the fluctuation of groundwater table in the future. Therefore, by predicting the groundwater level in Birjand aquifer, located in South Khorasan province, Iran, for the next 10 years under two

defined scenarios, an outline of the aquifer's behavior is estimated for the next ten years.

To this end, the present study uses the meshless local Petrov-Galerkin approach in Birjand aquifer for the first time, to predict the groundwater table in a real aquifer over a ten-year period. And also the parts of the aquifer most affected by these scenarios are identified and reported.

2. Methodology

2.1 The studied area

The studied area is Birjand aquifer with approximate coordinates of 32°34'-33°08' north latitude and 58°41'-59°44' east longitude. This unconfined aquifer has an approximate area of 269 km^2 and 30 m as an average saturation thickness (Mohtashami et al. 2019[18]; Sadeghi-Tabas et al. 2016[19]). Figure 1 shows the geographic location of the studied aquifer in Iran map.

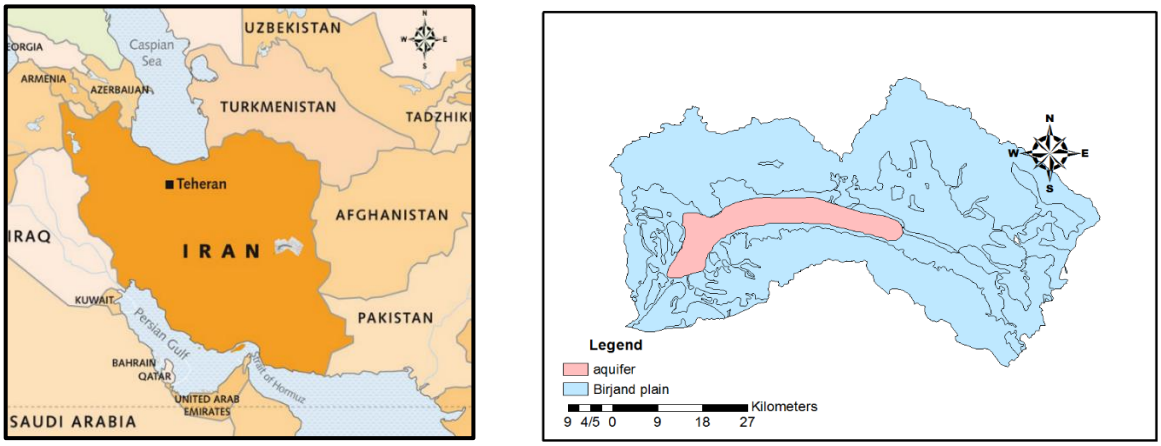

Fig. 1: The location of Birjand unconfined aquifer (red region in the right figure) in Birjand plain (blue region) in Iran map

It is noteworthy that there are 190 extraction wells and 10 observation wells in the aquifer, which are represented by the blue and red points in Figure 2, respectively. In Birjand aquifer, there are ten areas that have constant head boundary conditions. Figure 2 depicts these areas with black arrows.

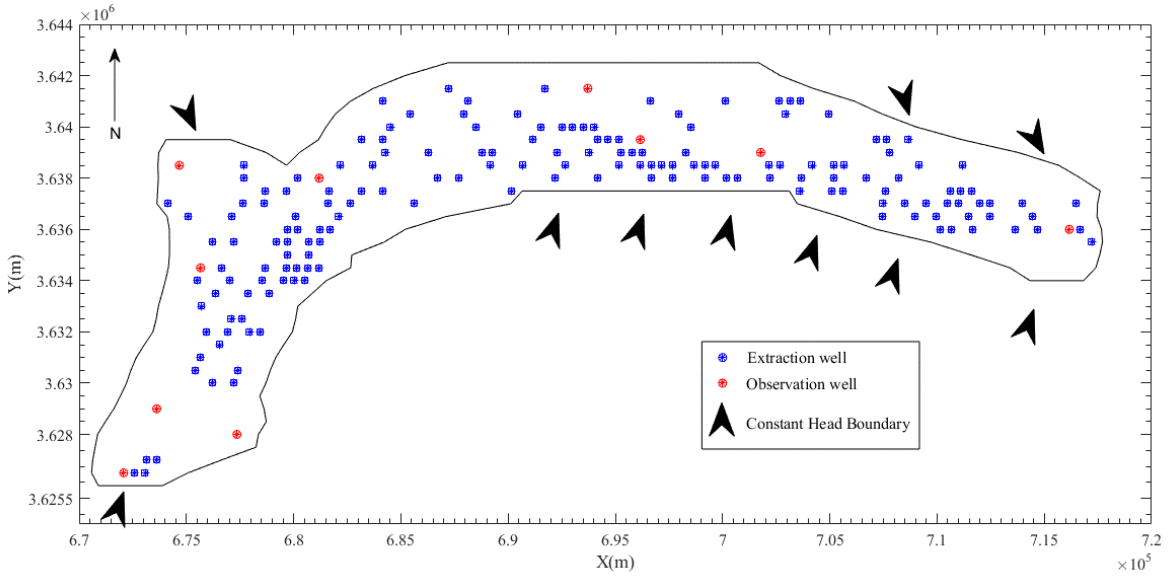

Fig. 2: The representation of the observation and extraction wells in Birjand aquifer

2.2 Governing equations of groundwater flow in an unconfined aquifer

In an unconfined aquifer, the governing equation for unsteady state is derived as Equation 1 based on both Dupuit assumption and continuity equations [20, 21].

$$\frac{\partial}{\partial x}\left(k_x H\frac{\partial H}{\partial x}\right)+\frac{\partial}{\partial y}\left(k_y H\frac{\partial H}{\partial y}\right) = \frac{S_y\partial H}{\partial t}+Q \times \delta(x-x_w)(y-y_w)+q \quad (1)$$

Where H is the groundwater level (m), k is the hydraulic conductivity coefficient (m/day) (k_x presents k in x-direction and k_y presents k in y direction), S_y is the specific yield, Q is the concentrated extraction or injection rate in cubic meter per day (with negative sign for extraction and positive sign for injection), and q is the distributed extraction or injection in square meter per day, e.g. evaporation (with a negative sign) and precipitation (with a positive sign).

It should be noted that as the equation is time-dependent (unsteady state), the initial conditions are obtained from the steady state analysis.

2.3 Meshless local Petrov-Galerkin (MLPG)

Several studies have been conducted on the development of meshless methods in fluid mechanics. Meshless methods eliminate the difficulties and problems of the sequential meshing and re-meshing only by adding and removing nodes in an appropriate position (Liu and Gu 2005[22]). In addition, it also reduces some of the limitations of the finite element method (FEM), which is related to updating boundary conditions. This problem causes significant errors when the domain has an irregular geometry (Profiri 2006[23]). In practice, meshless methods provide more accurate results with lower error than finite element method (Liu and Gu 2005[22]). Furthermore, it also remedies the shortcomings of the finite difference method (FDM), which is limited to rectangular grids and does not have enough flexibility to cover irregular geometry of the domains. In meshless modeling, certain nodes with known coordinates are scattered in the domain and its boundary. These nodes do not form a mesh [23].

The meshless local Petrov-Galerkin method, which is a weak form of the meshless methods (Liu and Gu 2005[22]), was first used by Aturiand Zhuin 1998 to solve the potential equation (Atluri and Zhu 1998[24]). This method, which is commonly used in the fluid field, utilizes two functions: a weight function and an approximation function. The moving kriging function is used as an approximation function to compute the shape function (∅) [7, 8].

2.4 Discretization of groundwater flow equation using the meshless local Petrov-Galerkin method

In order to solve the governing equation of the groundwater flow using the meshless local Petrov-Galerkin method, it is necessary to simplify the equations as follows.

$$\frac{\partial H^2}{\partial x}=2H\frac{\partial H}{\partial x}\ and\ \frac{\partial H^2}{\partial y}=2H\frac{\partial H}{\partial y} \quad (2)$$

Substituting Equation (2) into Equation (1) gives the following equation:

$$\frac{\partial}{\partial x}\left(k_x\frac{\partial H^2}{\partial x}\right)+\frac{\partial}{\partial y}\left(k_y\frac{\partial H^2}{\partial y}\right) = 2\times\left(\frac{S_y\partial H}{\partial t}+R\right). \quad (3)$$

which is:

$$R = Q\times\delta(x-x_w)(y-y_w)+q \quad (4)$$

Assuming a homogeneous and isotropic material for Birjand aquifer ($k_x = k_y$), Equation (5) is obtained as

$$k\left[\left(\frac{\partial^2 H^2}{\partial x^2}\right)+\left(\frac{\partial^2 H^2}{\partial y^2}\right)\right]=2\times\left(\frac{S_y\partial H}{\partial t}+R\right) \quad (5)$$

Finally, after discretizing according to the weighted residual method and divergence theorem, a set of linear equations of $KU = F$ appears.

The discrete form of each parameter is represented by Eq. (6)-(8) where K is stiffness matrix, F is Force body matrix, and U is an unknown matrix that shows groundwater level in each time period [26].

$$[K] = -2k\left[\iint_{\Omega}\frac{\partial W_i}{\partial x}H^n\frac{\partial \emptyset}{\partial x}d\Omega + \iint_{\Omega}\frac{\partial W_i}{\partial y}H^n\frac{\partial \emptyset}{\partial y}d\Omega\right] - 2\iint_{\Omega}W_i S_y\left(\frac{1}{\Delta t}\right)d\Omega \quad (6)$$

$$[U] = H^{n+1} \quad (7)$$

$$[F] = -2\iint_{\Omega}W_i S_y\left(\frac{H^n}{\Delta t}\right)d\Omega + 2\iint_{\Omega}W_i R d\Omega \quad (8)$$

in which, Ω and n represent the domain and time period, respectively.

In this study, the third-order spline weight function is computed with the following equation [25]:

$$W_i(X) = \begin{cases} \frac{2}{3}-4\overline{r_i^2}+4\overline{r_i^3}\,\overline{r_i} & \leq 0.5 \\ \frac{4}{3}-4\overline{r_i}+4\overline{r_i^2}-\frac{4}{3}\overline{r_i^3} & 0.5<\overline{r_i}\leq 1 \\ 0 & \overline{r_i}>1 \end{cases} \quad (9)$$

in which, $\overline{r_i}=\frac{d_i}{r_w}=\frac{|x-x_i|}{r_w}$ and r_w are the influence radius of node x_i. For each node, r_w must be selected in such a way that the number of non-zero weight functions be more than each term in the polynomial.

3. Result and Discussion

The meshless local Petrov-Galerkin method was used before to model groundwater flow in Birjand aquifer (Mohtashami et al. 2017[7-8]). The model was calibrated and verified and the results were more accurate and satisfactory than the results of the MODFLOW (Finite difference) model. Tables 1 and 2, which are derived from the reviewed studies, show the computed error indices in the steady and unsteady states, respectively.

Table 1. The computation of the error indices for steady state [7].

Error Indices	Finite Difference Method	Meshless Local Petrov-Galerkin
Mean Error (m)	0.321	0.234
Mean Absolute Error (m)	0.404	0.381
Root Mean Square Error (m)	0.566	0.483

Table 2. The computation of the error indices for unsteady state [8].

Error Indices	Finite Difference Method	Meshless Local Petrov-Galerkin
Mean Error (m)	0.159	-0.08
Mean Absolute Error (m)	1.434	0.573
Root Mean Square Error (m)	1.197	0.757

As shown in Tables 1 and 2, the meshless local Petrov-Galerkin method is more accurate than the Finite Difference method. Therefore, the predictions based on this model are more reliable and it can estimate the behavior of the aquifer in the future better than MODFLOW model, which uses Finite Difference method. The groundwater level, which is modeled based on the meshless local Petrov-Galerkin method without considering the scenarios, is illustrated in Figure 3.

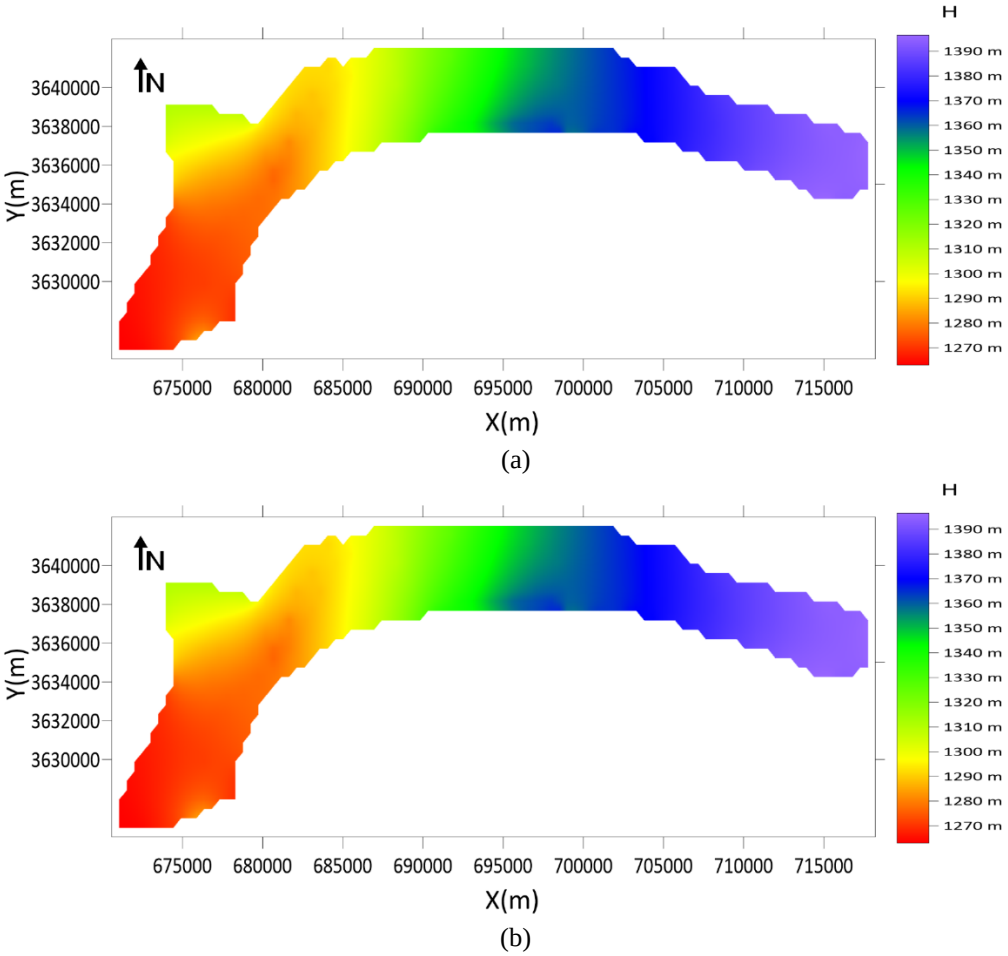

Fig. 3: The water table (a) at the beginning of the simulation and(b) at the last period of the simulation

As shown in Figure 3, the groundwater level in the eastern part of the aquifer is high (1398 m). As one moves from the east to the west of the aquifer, the groundwater level decreases remarkably so that the minimum groundwater level is located in the southwestern part of the aquifer (1263 m). In the northwestern part of the aquifer, which is shown in light green, the groundwater level is much higher than southern parts. This can happen for two reasons: (i)

closeness to the constant head boundary with high groundwater table, and (ii) low density of extraction wells in this area. This area is one of the ten areas of the aquifer that have constant head boundaries. In Figure 3, the changes in the groundwater level from the beginning of the simulation period (March 2011) to the end (March 2012) are evident. The slight difference in colors, especially in the western and southwestern parts of the aquifer, shows groundwater level changes during this one-year period with monthly time steps. The western part is shown in red at the beginning of the simulation period. The darker color of this part at the end of the simulation period indicates a decrement in the groundwater level.

The two scenarios used in this research are explained below.

3.1 Scenario 1: Constant precipitation rate with 10% increase in discharge rate compared to the previous year

Figure 4 shows groundwater levels at the end of a) the first year, b) the fifth year, and c) the tenth year. Groundwater level between those periods was depicted by interpolation.

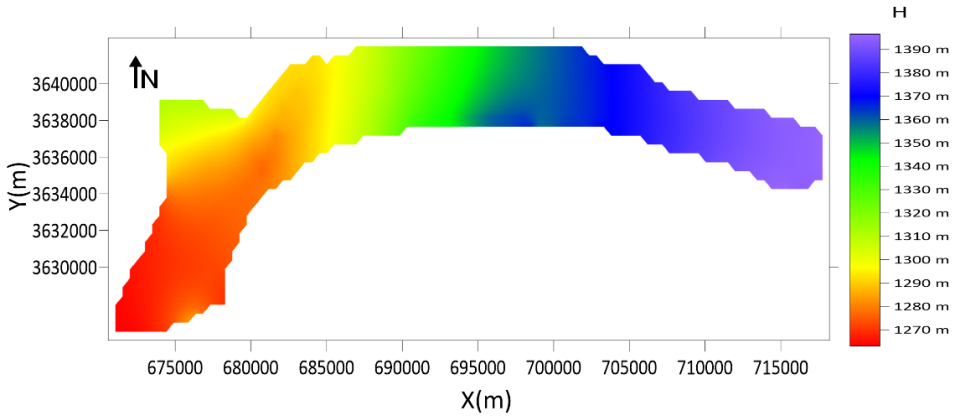

(a)

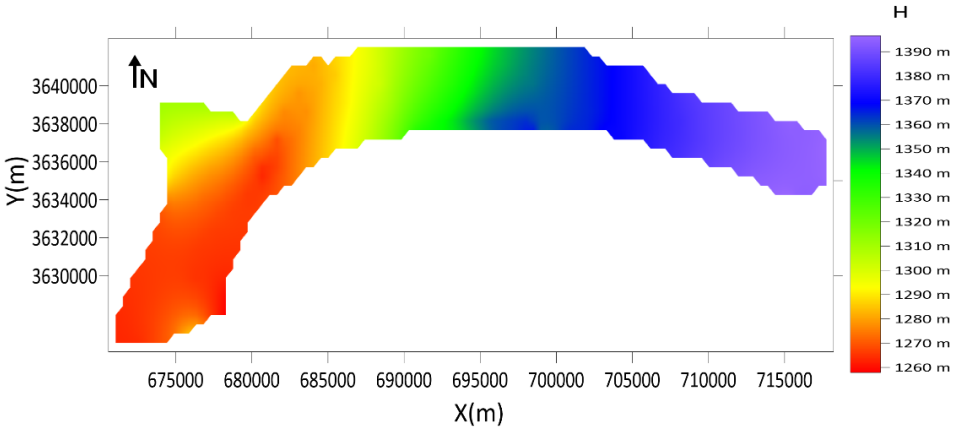

(b)

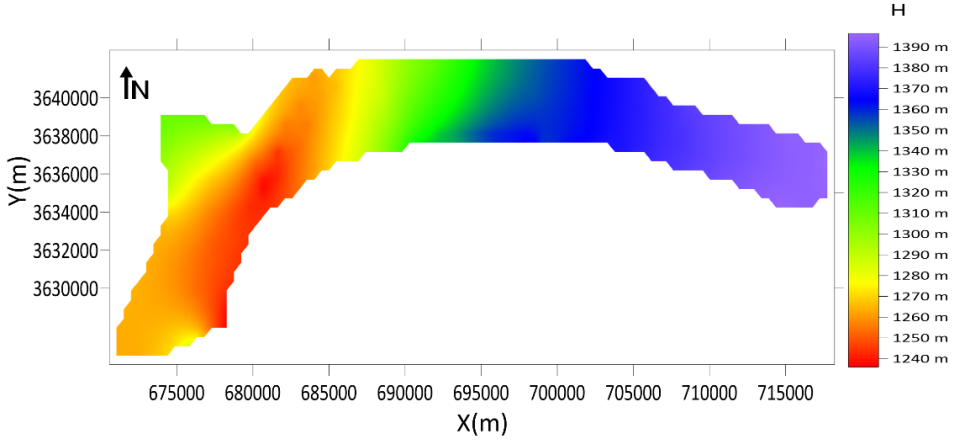

(c)

Fig. 4: Groundwater heads with the first scenario. a) At the end of the first year. b) At the end of the fifth year. c) At the end of the tenth year.

Regarding Figure 4a, the highest groundwater level is 1398 m located in the eastern part of the aquifer. The lowest groundwater table is located in the western and southwestern parts with a value of 1263.02 m. However, as Figure 4b shows, the lowest groundwater level is 1255.90 m and is located in the western part of the aquifer at the end of the fifth year. Figure 4c indicates that groundwater level declines as 14.55 m and 11.14 m in the western and central parts of the aquifer, respectively at the end of the tenth year. It should be noted that groundwater level decreases less in the eastern and central parts due to the low density of discharge wells in these parts of the aquifer. Another reason is that the pumping rate in these parts was lower than the pumping rate in the other parts of the aquifer. Meanwhile, there is an abrupt drawdown in the central part of the aquifer (in piezometer No. 8 location) due to the high density of groundwater wells such that the decline of groundwater level in this part of the aquifer in Figures 4b and 4c is 4.81 m and 11.14 m, respectively.

The groundwater levels in the locations of piezometers No. 5, 7, and 10 are obtained at the beginning and end of each year during the considered time period, and are presented in Figure 5.

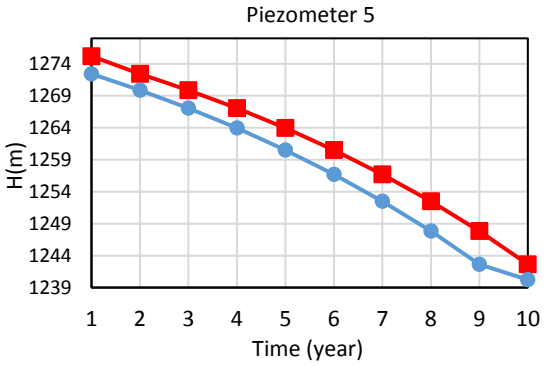

(a)

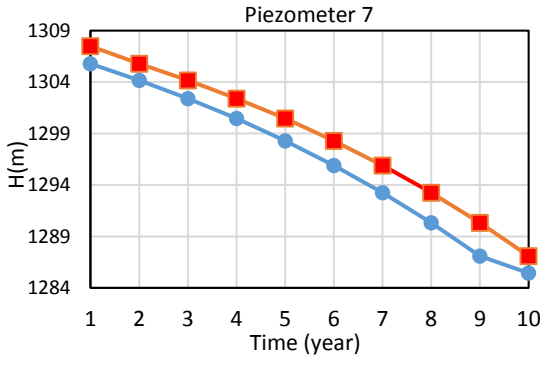

(b)

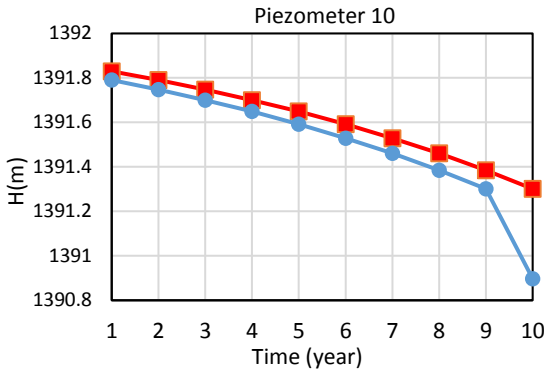

(c)

Fig. 5: The comparison of groundwater head at the beginning and end of the time period. (a) Piezometer 5; (b) Piezometer 7; and (c) Piezometer 10.

The red graph shows the values at the beginning of the time period and the blue graph corresponds to the end of the time period. According to Figure 5, the decreasing trend of the groundwater level in all graphs in each year is evident which is partly predictable since there is no change in the aquifer's recharge value such as rainfall.

Furthermore, the highest groundwater level corresponds to piezometer No. 10, which is located in the eastern part of the aquifer, in which the water drawdown at the end of the tenth year is 0.9 m compared to the beginning of the first year. Piezometers No. 5 and 7 experience 34.98 and 22.06 m drawdown in the groundwater level, respectively.

3.2 Scenario 2: A 5% increment in extraction rate of wells and a 20% decrement in rainfall rate compared to the year before

In this scenario, unlike the previous scenario, the effect of another variable, i.e. rainfall, is investigated. In addition to the 5% increment in the discharge rate, the value of rainfall is decreased by 20% compared to the year before. In other words, the rate of extraction increases and the recharge rate decreases. This scenario assumes a pessimistic situation. Figure 6 depicts the results at the end of years 1, 5, and 10.

In Figure 6a, the groundwater level is investigated at the end of the first year. In this case, the highest groundwater level is located in the eastern part of the aquifer and the lowest level is located in the southwestern part. In this case, the results do not significantly differ from Figure 4a, which was for the first scenario. The most drawdown occurs in the central part of the aquifer, which can be precisely detected by the color changes. Figure 6c, which corresponds to the end of the tenth year, shows a drop of 14.81 m in the southwest of aquifer (in the location of piezometer No. 5). Also, the center of the aquifer (in the location of piezometer No. 8) experiences a drawdown of 5.50 m.

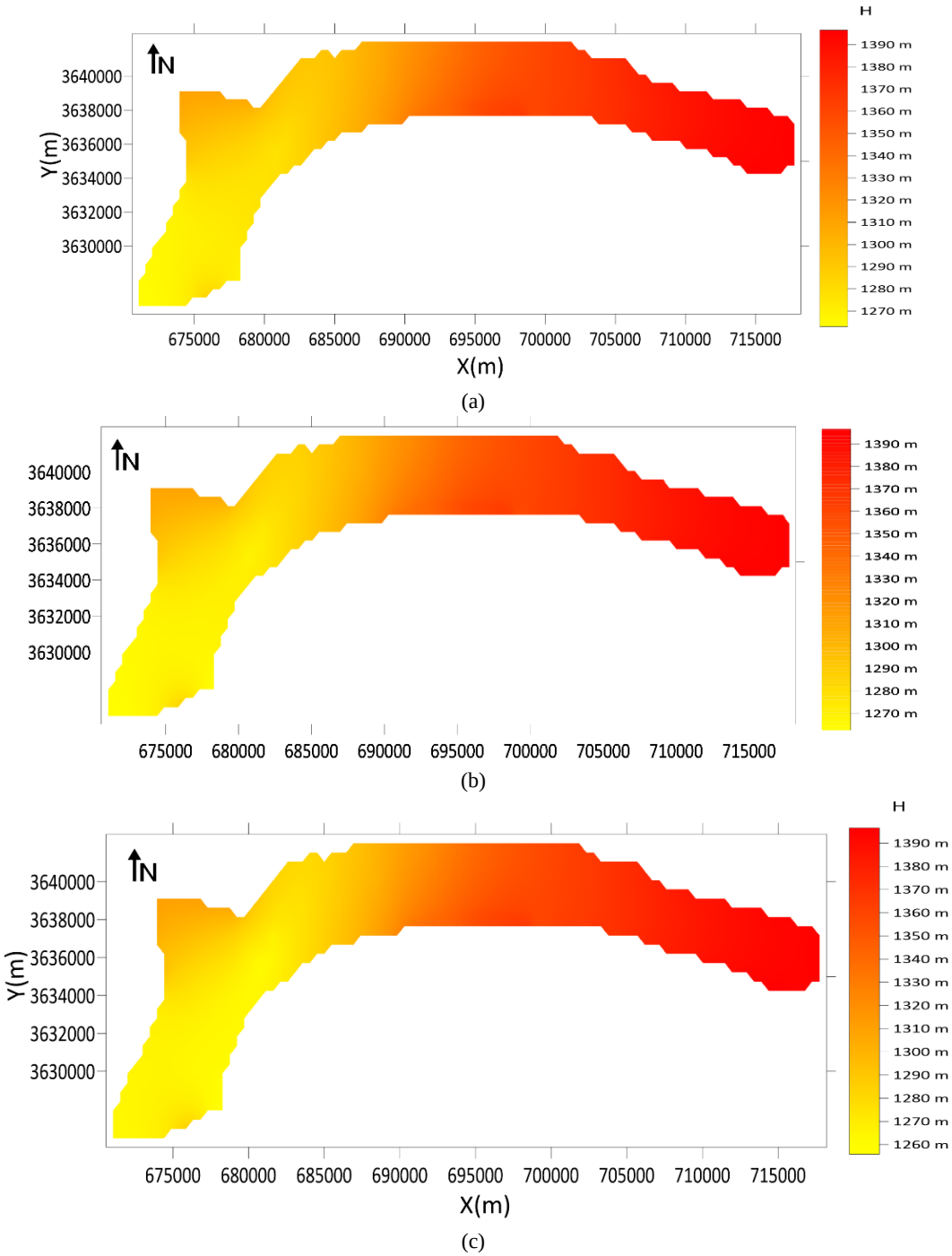

Fig. 6: Groundwater head under the second scenario. (a) The end of year 1; (b) The end of year 5; and (c) the end of year 10.

Conclusion

This study predicted the fluctuations of groundwater level in Birjand aquifer over a ten-year period for the first time. The studied aquifer is an unconfined aquifer in the Birjand plain located in South Khorasan province, Iran. The aquifer was modeled by meshless local Petrov-Galerkin numerical method. The model was calibrated and validated and the groundwater flow was simulated with two scenarios. The groundwater drawdowns were predicted during the simulation period. With the first scenario, an annual 10% increase was assumed in the discharge rate. The results of this scenario showed that the central and western parts of the aquifer would experience a drawdown of 11.74 and 35.80m, respectively. Then, taking the second scenario into account, the effect of precipitation was investigated as an additional variable. In this scenario the annual discharge rate was increased by 5%, and the annual precipitation rate was decreased by 20%. According to the results, at the end of the tenth year, the aquifer in the central and southern parts experienced a drawdown of 5.05 and 14.81 m, respectively.

References

[1] Nayak, P., SatyajiRao, Y., Sudheer, K., "Groundwater level forecasting in a shallow aquifer using artificial Neural Network Approach," Water Resources Management, vol. 20, 2006, pp. 77-90.

[2] Sreekanth, P. D., Sreedevi, P. D., Ahmed S., Geethanjali, N., "Comparison of FFNN and ANFIS models for estimating groundwater level," Environmental Earth Science, vol. 62, 2010, pp. 1301-1310.

[3] Prinos, S., Lietz A., Irvin, R., "Design of a real-time groundwater level monitoring network and portrayal of hydrologic data in southern Floria," US Geological Survey Report, Tallahassee, FL, 2002.

[4] Moosavi, V., Vafakhah, M., Shirmohammadi B., Behnia N., "Awavelet-ANFIS hybrid model for groundwater level forecasting for different prediction periods," Water Resources Management, vol. 27,2013 , pp. 1301-1321.

[5] Mategaonkar M., Eldiho, T. I., "Simulation of groundwater flow in unconfined aquifer using meshfree point collocation method." Engineering Analysis with Boundary Elements, Vol. 35,2011 , pp. 700-707.

[6] Boddula S., Eldho, T. I, "Groundwater flow simulation in confined aquifers using meshless Local Petrov-Galerkin," ISH Journal of Hydraulic engineering, Vol. 19,2013 , pp. 335-348.

[7] Mohtashami, A., Akbarpour, A., Mollazadeh, M., "Modeling of groundwater flow in unconfined aquifer in steady state with meshless local Petrov-Galerkin," Modarres Mechanical Engineering, vol. 17, no. 2, 2017, pp. 393-403.

[8] Mohtashami, A., Akbarpour, A., Mollazadeh, M., "Development of two dimensional groundwater flow simulation model using meshless method based on MLS approximation function in unconfined aquifer in transient state," Journal of Hydroinformatics , vol. 19, no. 5, 2017,pp. 640-652.

[9] Wen, X. H., Wu, Y. Q., Lee, L. J. E., Su, J. P., Wu, J., "Groundwater flow modeling in the Zhangye Basin, Northwestern China," Environmental Geology, vol. 53, no. 1, 2007 ,pp. 77-84.

[10] Shiri, J., Kisi, O., Yoon, H., Lee, K.-K., Nazemi, A. H., "Predicting groundwater level fluctuations with meteorological effect implications—A comparative study among soft computing techniques," Computers & Geosciences, vol. 56, 2013,pp. 32-44.

[11] Cortes, C., Vapnik, V., "Support-vector networks. Machine learning," Machine Learning, 1995 ,pp. 273-297.

[12] Shirmohammadi, B., Vafakhah, M., Moosavi, V., Moghaddamnia, A., "Application of Several Data-Driven Techniques for Predicting Groundwater Level," Water Resources Management, vol. 27, 2013 ,pp. 419-432.

[13] Emamgholizadeh, S., Moslemi, K., Karami, G., "Prediction the Groundwater Level of Bastam Plain (Iran) by Artificial Neural Network (ANN) and Adaptive Neuro-Fuzzy Inference System (ANFIS)," Water Resources Management, vol. 28, no. 15, 2013 ,pp. 5433-5446.

[14] Ghafarian, A., Groundwater flow simulation with MODFLOW and land susidance estimation in Kashmar plain, Mashhad: Ferdowsi University of Mashhad, 2013.

[15] Nikbakht, J., Najib, Z., "Effect of irrigation efficiency increasing on groundwater level fluctuations (Cast study: Ajab-Shir Plain, East Azarbaijan)," Journal of Water and Irrigation Management, vol. 5, no. 1, 2015, pp. 115-127.

[16] Ghobadian, R., Bahrami, Z., Dabagh Bagheri, S. , "Applying the management scenarios in prediction of groundwater level fluctuations by using the conceptual and mathematical MODFLOW model (Case study: Khezel-Nahavand Plain)," Iranian Journal of Ecohydrology, vol. 3, no. 3, 2016 ,pp. 303-319.

[17] Yousefi Sahzabi, H., Zahedi, S., Niksokhan, M. H., "Ten Year Prediction of Groundwater Level for the Purpose of of Determining Reasonable Policies for Exploitation from Aquifer," Iranian Journal of Ecohydrology , vol. 3, no. 3, 2016,pp. 405-414.

[18] Mohtashami, A, Hashemi Monfare, S. A., Azizyan, G., Akbarpour, A., "Determination the capture zone of wells by using meshless local Petrov-Galerkin numerical model in confined aquifer in unsteady state(Case study: Birjand Aquifer)," Iranian Journal of Ecohydrology, vol. 6, no. 1, 2019 ,pp. 239-255.

[19] Sadeghi Tabas, S., Samadi, S. Z., Akbarpour, A., Pourreza Bilondi, M., "Sustainable groundwater modeling using single-and multi-objective optimization algorithms.", Journal of Hydroinformatics, Vol. 18, no. 5, 2016, pp. 1-18.

[20] Dupouit, J., Estudes Theoriques et Pratiques sur le Mouvement desEaux, Paris: Dunod, 1863.

[21] Todd, D. K., Mays, L. W., "Groundwater hydrology edition." Welly Inte, 2005.

[22] Liu, G. R., Gu, Y. T., An introduction to Meshfree Methods and Their Programming, Singapore: Springer, 2005.

[23] Porfiri, M., Analysis by Meshless Local Petrov-Galerkin Method of Material Discontinuities, Pull-in Instability in MEMS, Vibrations of Cracked Beams, and Finite Deformations of Rubberlike Materials, Virginia: Virginia Polytechnic Institute and State University, 2006.

[24] Atluri, S. N., Zhu, T. A., "A new MEshless method (MLPG) approach in computational mechanics," Computational Mechanics, vol. 22, no. 2, 1998,pp. 117-127.

[25] Liu, G.R., Mesh Free Methods: Moving Beyond the Finite Element Method. Boca Raton: CRC Press, 2002.

[26] Mohtashami, A, Hashemi Monfared, S. A., Azizyan, G., Akbarpour, A., " Determination of the optimal location of wells in aquifers with an accurate simulation-optimization model based on the meshless local Petrov-Galerkin," Arabian Journal of Geosciences, (Submitted)

[27] Shabani, A., Asgarian, B., Asli Gharebaghi, S., Salido M. A, Giret A., "a new optimization algorithm based on the search and rescue operations", Mathematical problems in Engineering (accepted)